International Journal of Nanomedicine

Dovepress
Taylor & Francis Group

Open Access Full Text Article

ORIGINAL RESEARCH

Mir-218-5p from Extracellular Vesicles of Endometrium in Patients with Recurrent Implantation Failure Impairs Pre-Implantation Embryo Development

Lei Cai[1,*], Mingwei Lv[2,3,*], Jianbo Wei[1], Chang Liu[4], Yuehan Li[1], Zhiqi Liao[1], Tianhui Li[5], Hanwang Zhang[1], Ling Xi[2,3], Cong Sui[1]

[1]Reproductive Medicine Center, Tongji Hospital, Tongji Medical College, Huazhong University of Science and Technology, Wuhan, 430030, People's Republic of China; [2]Department of Gynecological Oncology, Tongji Hospital, Tongji Medical College, Huazhong University of Science and Technology, Wuhan, People's Republic of China; [3]National Clinical Research Center for Obstetrics and Gynecology, Cancer Biology Research Center, Key Laboratory of the Ministry of Education, Tongji Hospital, Tongji Medical College, Huazhong University of Science and Technology, Wuhan, People's Republic of China; [4]Reproductive Medicine Center, Department of Obstetrics and Gynecology, Nanjing Drum Tower Hospital, The Affiliated Hospital of Nanjing University Medicine School, Nanjing, 210000, People's Republic of China; [5]State Key Laboratory of Digestive Disease, Li Ka Shing Institute of Health Sciences, Department of Medicine and Therapeutics, The Chinese University of Hong Kong, Hong Kong

*These authors contributed equally to this work

Correspondence: Cong Sui, Email csui0904@163.com

Background: Recurrent implantation failure (RIF) presents a crucial obstacle to in vitro fertilization success. Previous research has shown that small extracellular vesicles (EVs) from endometrial RIF patients hinder embryo development, yet the underlying mechanism and potential solutions remain largely unexplored. In this study, we aimed to investigate the effectiveness of miR-218-5p as a molecular factor in RIF-EVs. Our findings revealed that miR-218-5p disrupted mouse embryo development, and this effect could be reversed by engineered extracellular vesicles (E-EVs) containing anti-miR-218-5p.

Methods: The percentage of blastocyst development and hatching rates, embryo morphology, and the total cell number were measured. RNA-sequencing was used to analyze transcriptional changes in embryos post miR-218-5p agomir treatment. The abnormal segregation genes of trophectoderm (TE) and inner cell mass (ICM) were visualized via qRT-PCR and immunofluorescence staining. The E-EVs were using the EVs derived from Human Umbilical Cord Mesenchymal Stem Cells (HUMSCs). Characteristics of the EVs were measured using Western blotting, nanoparticle tracking analysis, and transmission electron microscopy. EVs internalization was visualized using BODIPY TR ceramide staining.

Results: Mouse embryos were arrested at the morula stage and demonstrated reduced blastocyst and hatching rates following miR-218-5p agomir treatment ($P < 0.001$). Essential transcription factors for TE and ICM, such as Cdx2, Yap1, Sox2, Nanog, Tead4, were reduced at the mRNA level in the miR-218-5p treated morula. This was accompanied by decreased Cdx2 protein levels at the 8–16-cell stage ($P < 0.001$) and disruption of co-localization of Yap1 and Cdx2. The blastocyte rate was increased by anti-miR-218-5p-encapsulated E-EVs compared with miR-218-5p group ($P < 0.001$).

Conclusion: This study offers valuable insights into the potential role of miR-218-5p in RIF and presents. The utilization of engineered vesicles containing anti-miR-218-5p may present a promising avenue for patients facing challenges with RIF.

Plain Language Summary: The phenomenon of recurrent implantation failure (RIF) is a common occurrence in patients undergoing the assisted reproductive technology (ART) process. It intensifies the strain on patients, but as of now, there is no universally accepted definition, cause, or therapeutic strategy. RIF can result from various factors, and recently, the impact of small vesicles released from cells called extracellular vesicles (EVs) has garnered increasing attention in the disease process of RIF. However, there is still a lack of mechanistic evidence and therapeutic recommendations. In this study, we discovered that miR-218-5p is one of the functional molecules inside the RIF-EVs, and it disrupts the development of the embryo into a blastocyst. Furthermore, we found a deeper mechanism related to the distribution of the formation of the trophectoderm (the embryo's outer cell). This provides a plausible

Received: 10 December 2024
Accepted: 23 April 2025
Published: 1 May 2025

Graphical Abstract

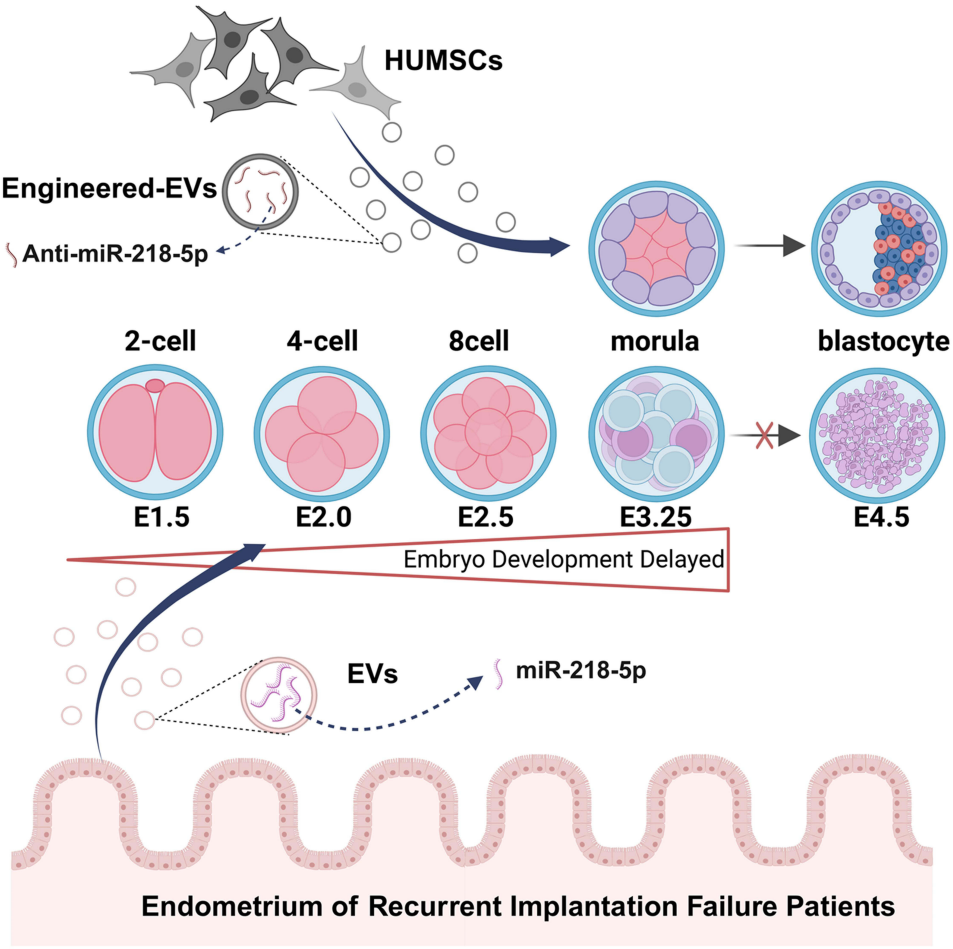

explanation for one form of embryonic disorder associated with RIF. Most significantly, our work introduces a novel therapeutic approach, employing engineered EVs encapsulating anti-miR-218-5p, which effectively mitigates the deleterious effects of miR-218-5p. This research provides a novel and non-invasive insight into potential therapeutic strategies for RIF.

Keywords: recurrent implantation failure, extracellular vesicles, microRNA, pre-implantation embryo, engineered extracellular vesicles

Introduction

Assisted reproductive technology (ART) provides an alternative opportunity for couples unable to conceive naturally due to various etiologies.[1] However, recurrent implantation failure (RIF) is a common issue during ART, significantly impacting the mental and financial well-being of affected families.[1–4] RIF is a complex condition, involving factors such as the maternal immune system, the aneuploid embryos, the unsynchronized embryo-endometrial interactions, and the imbalanced reproductive tract microenvironment.[5–7] Understanding the underlying mechanisms of RIF and developing effective treatment strategies is crucial.

Extracellular vesicles (EVs) are nanosized biological particles that transport molecular cargo, including microRNAs (miRNAs), proteins, and lipids, intercellularly and across tissues.[8,9] EVs in the microenvironment of the female

reproductive tract mediate the embryos-maternal cross-talk process.[10] They exhibited divergently proteomic and pro-transcriptional profiles that are phase-specific during the menstrual cycle.[11,12] We focused on the EVs from RIF patients' endometrial cells during the window of implantation (WOI), the prerequisite period for successful implantation.[13,14] Our former research constructs the consequence that blastocyte formulation was impaired after co-culturing with WOI-endometrial EVs of RIF patients in vitro.[15] However, the current explanation of the effectiveness of the RIF-EVs in the embryos is limited since most of the transcripts are under bioinformatic analysis only.[11,16–18] The identification of the causes of the RIF-EVs disturbed embryo development requires a deeper understanding of the molecular mechanisms.

Among all the components in the EVs, miRNAs, the small non-coding RNAs that regulate gene expression post-transcriptionally, are considered one of the major functional molecules.[19,20] The miRNA patterns in EVs, originating from endometrial cells, organoids, and uterine fluid, exhibit distinct variations throughout the menstrual cycle.[18,21–23] Our previous study revealed the altered miRNA profiles in RIF-EVs.[18] Similarly, Carolina et al reported variations in miRNA profiles in the WOI uterine fluid of RIF patients.[24] These results indicate that the composition of miRNAs in women with RIF deviates from that of healthy fertile women. Furthermore, these variations imply that maternal miRNAs have a widespread presence throughout both physiological and pathological processes. In addition to the embryonic miRNA, whose distribution is linked to embryonic abnormalities and infertility,[25–27] it is also established that the maternal miRNAs affect the pro-implantation embryo development at the post-transcriptional level ranging from the zygote to the blastocyst stage.[28–31] Several miRNAs have been reported to modulate early-stage embryo development, for example, miR-212 silences the transcription factor in the germline alpha leading to a halt in embryo at the 8-cell,[32] and miR-218 can impede the progression of bovine morula embryos to the blastocyst stage.[33,34] The miRNAs represent diverse gene patterns in the cargo of the pre-receptive or receptive-phase endometrium EVs, which are highly related to uterus receptivity and embryo development.[35] Our previous research employed miRNA sequencing analysis and validated that miR-218-5p, miR-1246, and miR-6131 were up-regulated in RIF-EVs.[18] However, there is still a lack of research on the impact of those three miRNAs on pre-implantation. The specific miRNA pattern of RIF-EVs emphasizes the importance of understanding the role of these molecules in RIF. To investigate whether the presence of miRNAs in RIF-EVs affects embryo development, we co-cultured embryos with miR-218-5p, miR-1246, and miR-6131 and identified miR-218-5p as a critical molecule in the process of pre-implantation embryonic development. We aim to elucidate the impact of RIF-EVs containing miR-218-5p on embryo development and the underlying mechanisms. Moreover, we explore the potential therapeutic application of engineered extracellular vesicles (E-EVs) encapsulating anti-miR-218-5p to counteract the detrimental effects of RIF-EVs. E-EVs are considered novel vesicles with slight allograft rejection and high targeting ability.[36] This research seeks not only to enhance our understanding of the molecular mechanisms involved in RIF but also to lay the groundwork for the development of innovative treatment strategies targeting these mechanisms.

Materials and Methods

Animals and Mouse Superovulation

Institute of Cancer Research (ICR) mice (female 6–10 weeks old, male 8–20 weeks) were kept in the Animal Center of Tongji Hospital, with regulated temperature conditions, 12 hours light-dark cycle and libitum water and food. All animal experiments were approved by the Medical Ethics Committee of Tongji Medical College, Huazhong University of Science and Technology (2022S067) and followed the National Institutes of Health guide for the care and use of laboratory animals (NIH Publications No. 8023, revised 1978). All female mice were intraperitoneally injected with 5 IU pregnant mare's serum gonadotropin (PMSG, Sigma-Aldrich, St. Louis, USA) at 5–6 pm and followed by 5 IU hCG (Sigma-Aldrich) injection 48 hours later. The mice underwent ovarian stimulation were mated in a male:female ratio of 1:2 after the hCG injection immediately, and the vaginal plug were checked next morning.

Mouse Embryo Culture

The 2-cell stage embryos from the female mice oviduct were collected in M2 medium (M7167, Sigma-Aldrich) after 36–40 h hCG injection and cultured in the CZB medium (MR019, Sigma-Aldrich) covered by mineral oil (M5310, Sigma-Aldrich) in a triple gas incubator (6% CO2, 89% N2, and 5% oxygen) at 37°C. The embryos were co-cultured

with miRNA agmoir at E2.0 (4-cell-stage, zygote is considered as embryo day E0.5), 54–55 hours after the hCG injection. Agmoir or anti-miR-218-5p were diluted with CZB medium at 3 nM and the mini-drops were pre-incubated for 2 hours before embryo culture, and each droplet under 50 uL volume, contained 5–10 embryos from at least three mice. The 8-cell, morula and blastocyte rate were counted at E2.5, E3.25 and E 4.5, respectively.

RNA Extraction and Quantitative Real-Time Polymerase Chain Reaction

The total RNA of the embryos was extracted using the Dr. GenTLE Precipitation Carrier kit (NO. 9094, TaKaRa, Japan) following the manufacturer's instructions. For the miRNA detection, synthesis cDNA and quantitative real-time polymerase chain reaction (q-RT-PCR) were using the All-in-one miRNA qRT-PCR Detection Kit (QP015, GeneCopoeia, Guangzhou, China), and 100 ng total RNA was used to synthesize cDNA. The expression of miRNA was normalized by miR-U6. For the mRNA detection, the embryos were reversed using Single-Cell Sequence Specific Amplification Kit (P621-249 01, Vazyme, Nanjing, China). The q-RT-PCR analysis was performed using the ChamQ Universal SYBR qPCR Master Mix (Q711, Vazyme) and a Roche Light Cycler 480 Instrument II PCR System. The relative expression of mRNA was calculated by normalization to the GAPDH mRNA levels, using the $2^{-\Delta\Delta Ct}$ method. Each experiment was performed triple. The details of the primer information are listed in Table 1.

RNA-Seq Library Construction and Deep Sequencing

The cDNA from each sample was transcript reversed by the Smart Seq2 and checked by Qubit® 3.0 Fluorometer and Agilent 2100 Bioanalyzer to ensure the production with length around 1~2kbp. Seven to ten compacted embryos at E3.25 from at least three different mice constituted one sample of miR-218-5p and miR-NC groups, respectively. The RNA-Seq library was prepared following the Illumina library preparation protocol,[37] then loaded onto the Illumina HiSeq platform for PE150 sequencing.

RNA Seq Data Analysis

The DEGs between miR-218-5p and miR-NC groups were defined as log2 |fold change|>1 and Benjamin–Hochberg corrected *P*-value ≤ 0.05 with DESeq2 R package. The Gene Ontology (GO) and Kyoto Encyclopedia of Genes and Genomes (KEGG) pathway enrichment analysis based on the calculated DEGs were annotated with Bonferroni-corrected *P*-value ≤ 0.05, using the Goatools (https://github.com/tanghaibao/Goatools) and KOBAS (http://kobas.cbi.pku.edu.cn/home.do). The Volcano plots and the heatmap were constructed with DEGs using the R platform.

Table 1 Primer Sequence

Primer Name	Primer Sequence
miR-218-5p	TTGTGCTTGATCTAACCATGTAAA
miR-6131	GGCTGGTCAGATGGGAGTGA
miR-U6	CGCTTCACGAATTTGCGTGTCAT
Nanog-F	TTCTGGGAACGCCTCATC
Nanog-R	GCTTTTGTTTGGGACTGG
Tead4-F	TTGGAGTTCTCGGCTTTC
Tead4-R	TCATAGATTTGGCGGATG
Cdx2-F	GGAAAATCAAGAAGAAGCA
Cdx2-R	AGGTCACAGGACTCAAGG
Gapdh-F	GGTGAAGGTCGGTGTGACCG
Gapdh-R	CTCGCTCCTGGAAGATGGTG
Yap1-F	GCAATACGGAATATCAATC
Yap1-R	TGCCACTGTTAAGAAAGG

Immunocytochemistry

Embryos from the various developmental stages were fixed with 4% paraformaldehyde (PFA) for 30 minutes. The fixed embryos were permeabilized with 0.5% Triton X-100 for 20 minutes, then blocked with 10% FBS (Thermo Fisher Scientific, CA, USA) with PBT 0.1% Triton X-100 for 2 hours at room temperature. The primary antibody was incubated over night at 4°C, and washed three times in blocking buffer next day following the incubation with secondary fluorescent antibody for 1 h at room temperature (RT). The detailed concentration of antibodies was listed: Cdx2 (12306, 1:200 diluted, Cell Signaling Technology, Danvers, MA, USA), Yap1 (14074, 1:200 diluted, Cell Signaling Technology), Goat Anti-Mouse IgG (ab150117, 1:500 diluted Abcam), FlexAble CoraLite® Plus 555 Antibody Labeling Kit for Rabbit IgG (KFA002, Proteintech, Planegg-Martinsried, Germany). DNA was dyed with 4 μg/mL Hoechst 33258 staining dye solution (Servicebio, Wuhan, China) for 30 min at RT. All images of the samples were captured by the laser scanning confocal microscope (Dragonfly/CR-DFLY-201-40, ANDOR, UK).

EdU

The proliferation of the blastomere was detected by the Cell-Light™ EdU Apollo in vitro Kit (RIBOBIO, Guangzhou, China) following the manufacturer's instructions. In brief, the miR-218-5p treated morula was incubated with 5-Ethynyl-2′-deoxyuridine (EdU) in a triple gas incubator at 37°C for 2h, then fixed with 4% PFA. The fixed morula was stained by 1×Apollo reaction buffer and Hoechst 33258 then imaged by fluorescence microscope.

TUNEL Assay

The terminal deoxynucleotidyl transferase dUTP nick end labeling (TUNEL) assay was used to detect the apoptosis of embryos from miR-218-5p and miR-NC groups, with TMR (red) Cell Apoptosis Detection Kit 242 (G1501, Servicebio) according to the manufacturer's instructions. The labeled embryos were mounted onto glass slides, under glass cover slips, in a drop of anti-fade reagent (G1401, Servicebio). The apoptosis cell number was counted.

ROS Analysis and Mitochondrial Staining

The intracellular ROS levels in the 8-cell embryos stage were detected using a ROS assay kit (S0033S, Beyotime, Shanghai, China) according to the manufacturer's protocol. The activity of mitochondria in the morula at E3.25 was evaluated using Enhanced mitochondrial membrane potential assay kit with JC-1 (C2003S, Beyotime) according to the manufacturer's protocol. A fluorescence microscope (Axio Observer A1, Carl221 Zeiss, Germany) was used to image the embryos, and the fluorescence intensity was analyzed based on ImageJ software.

Human Umbilical Cord Mesenchymal Stem Cells Cultural and EV Isolation

Human Umbilical Cord Mesenchymal Stem Cells (HUMSCs) were provided by Warner Bio technology (Wuhan, China), cells were cultured in DMEM/F12 (Thermo Fisher Scientific) with 10% FBS (Thermo Fisher Scientific) and 1% penicillin/streptomycin (Thermo Fisher Scientific) at 37°C and 5% CO_2 in a humidified incubator. Flow cytometry was used to identify related surface markers using HLA-DR (Cat. No. 307603, BioLegend, US), CD34 (Cat. No. 560942, BDbio), CD45 (Cat. No. 304005, BioLegend), CD44 (Cat. No. 561858, BDbio), CD73 (Cat. No. 344003, BioLegend), CD90 (Cat. No. 328109, BioLegend), CD105 (Cat. No. 800503, BioLegend) in 1:500 diluted. To isolate MSC-EVs, HUMSCs were rinsed twice with PBS, cultivated in 10% Exo-free-FBS in DMEM/F12 medium (Thermo Fisher Scientific) for 48 hours, and the supernatant was collected for EV extraction. The EV isolation protocol used the classic ultracentrifugation method.[15,38,39] Briefly, centrifuge the medium at 300 g (10 min), 2000 g (10 min), and 10,000 g (30 min) at 4°C to remove cells, dead cells, and debris. Filter the supernatant with 0.22 μm, followed by the 90 min 100,000 g ultracentrifugation. The pellet was resuspended in PBS, repeated 100,000 g ultracentrifugation, then resuspend in 50 μL PBS and stored at −80°C.

Nanoparticle Tracking Analysis (NTA)

The diameter and distribution of EV were analyzed by nanoparticle tracking analysis (NTA, ZetaView Metrix, Germany). Samples were diluted in ddH_2O to reach the ideal particle per frame value (100–200 particles/frame). All samples setting as the same sensitivity following the manufacturer's default software settings.

Transmission Electron Microscopy (TEM)

The 10 μL of fresh EVs was pipetted onto a 400-mesh copper grid with carbon-coated formvar film and incubated for 2 min and removed extra liquid. The grid was briefly placed on 10 μL of uranyl acetate and washed twice with 100 μL MilliQ water. Dried EVs-attached grids were observed by Tecnai G220 High Resolution Transmission Electron Microscopy, FEI, US.

Western Blot

HUMSCs were rinsed in IP lysis buffer for 30 minutes on ice, centrifuged at 12,000 g for 15 minutes at 4°C. The concentration of both EVs and HUMSCs lysates protein were analyzed by *DC* Protein Assay Reagents Package (Bio-Rad Laboratories, Delaware, USA) followed by the manufacturer's protocol. Each sample was boiled at 100°C 5 min and separated (10 μg) via sodium dodecyl sulfate–polyacrylamide gel electrophoresis (SDS-PAGE) then transferred to a polyvinylidene fluoride membrane (Millipore). Membranes were blocked in 5% skimmed milk then incubated with primary antibodies overnight at 4°C, followed by appropriate horseradish peroxidase-conjugated secondary antibodies incubation 1 h at RT for bands signal detection. The primary antibodies were added at 1:1,000 dilution and listed: TSG101 (ab125011; Abcam, Cambridge, MA, USA), CD9 (A1703, ABclonal), CD63 (ab134045, Abcam), CD81 (27855-1-AP, proteintech), Calnexin (2679; Cell Signaling Technology)

Engineered Small Extracellular Vesicles Packaging

The peptide-based method[40] was used to load the anti-miR-218-5p into the HUMSC derived EVs. In brief, 300 pmol of the anti-miR-218-5p, Exosome-Transit Peptide (ETP) (ExoLoad®, Echobiotech, China) and 100 μL EVs (3×10^{12} particles/mL) were added in the reaction buffer, incubated at 37°C in the dark for 2 hours with continuously shaking (150 rpm). Removed the free nucleic acid and peptide in the buffer by washing with PBS in a 100 kDa Amicon Ultracentrifugal filter (Merck Millipore, Billerica, MA, USA) centrifuge at 2000 g until the volume is reduced to 100 μL (1×10^{12} particles/mL). Added the approximate volume of packaged E-EVs into the CZB (MR019, Sigma-Aldrich) embryo culture medium to reach the final concentration 2×10^{10} particles/mL and pre-warm 2 h.

Embryo EV Uptake Assay

Added 100 μL (1×10^{12} particles/mL) EVs or E-EVs with 1 μL BODIPY TR ceramide (Thermo Fisher Scientific) incubate at 37°C in the dark for 20 min, followed by the 90 min 100,000 g ultracentrifugation. The pellet was resuspended in PBS, repeated ultracentrifugation to obtain the stained EV. Added the stained EVs into the CZB (MR019, Sigma-Aldrich) embryo culture medium. After 2 hours pre-warm, transfer the 4-cell embryos into the pre-incubated droplets, co-cultured the embryos with the stained EV for 10 h then fixed the embryos with 4% PFA for 30 minutes. After 30 min Hoechst 33258 staining (Servicebio), fixed embryos were imaged using fluorescence microscopy (Zeiss, Germany).

Statistical Analysis

Quantitative variables were presented as mean ± standard deviation (SD). The data were subjected to Student *t* test to evaluate statistical significance between miR-218-5p and miR-NC groups. The 8-cell rate, morula rate, blastocyte rate, and hatching rate were conculcated by the Chi-square tests followed by Bonferroni tests. For all the statistical analysis, $P < 0.05$ was considered statistically significant.

Results

Effects of miRNAs in RIF-EVs on Embryonic Development

To investigate the functional impact of specific miRNAs on mouse blastocyst formation mediated by RIF-EVs, we conducted in vitro embryo culture experiments involving three up-regulated miRNAs previously identified in our research: miR-218-5p, miR-1246, and miR-6131. The blastocyte and hatching rates were significantly decreased after miR-218-5p treatment, but remained unchanged with miR-1246 and miR-6131 agomir (Figure 1A, B and Supplemental Figure 1). After miRNAs agomir treatment, the blastocytes were highly expressed in the miR-218-5p (Figure 1C). Bright fields of mice embryos are displayed in Figure 1D. The miRNA expression in mice embryos was stage-dependent.[41–43] Our results indicated that the expression of the miR-218-5p, miR-1246 and miR-6131 was increased markedly at the 8-cell stage and restricted at the blastocysts (Supplemental Figure 2), while the expression of those miRNAs was relatively high at blastocyst after agomir treatment (Figure 1C).

Impaired Mouse Blastocyst Formation After the miR-218-5p Treatment

To identify the most reliable candidate miRNA for disrupting embryo development, further experiments concentrated on miR-218-5p, which demonstrated the highest expression among the effective miRNAs.[18] Mouse embryos were cultured with miR-218-5p agomir, which demonstrated the highest expression among the effective miRNAs in RIE-EVs,[18] from E2.0 until the late blastocyst stage and monitored the developmental process at E2.5 (8-cell-stage), E3.25 (morula-stage), E4.5 (blastocyte-stage), and E5.5, respectively. As shown in Table 2, the 8-cell embryo formulation rate and the compaction rate at E2.5 and E3.25 were lower in the miR-218-5p groups less compared to the NC group ($P < 0.001$), respectively. At the general blastocyst formulation stage E4.5, there was a significantly decreased blastocyst rate after miR-218-5p treatment ($P < 0.001$), while more than half of the embryo can reach to morula stage at E4.5 (52.3%). We prolonged the culture to E5.5, there was no significant increase in the blastocyst rate of the miR-218-5p group when comparing E4.5 ($P = 0.274$). Nevertheless, there was a noticeable increase in the collapse rate at E5.5 in the miR-218-5p group ($P < 0.01$). As shown in Figure 2A, embryos failed to form a cavity and appeared to collapse at the late blastocyst stage (E5.5). Those observations suggested that the delay of compaction was presented in miR-218-5p agomir treatment

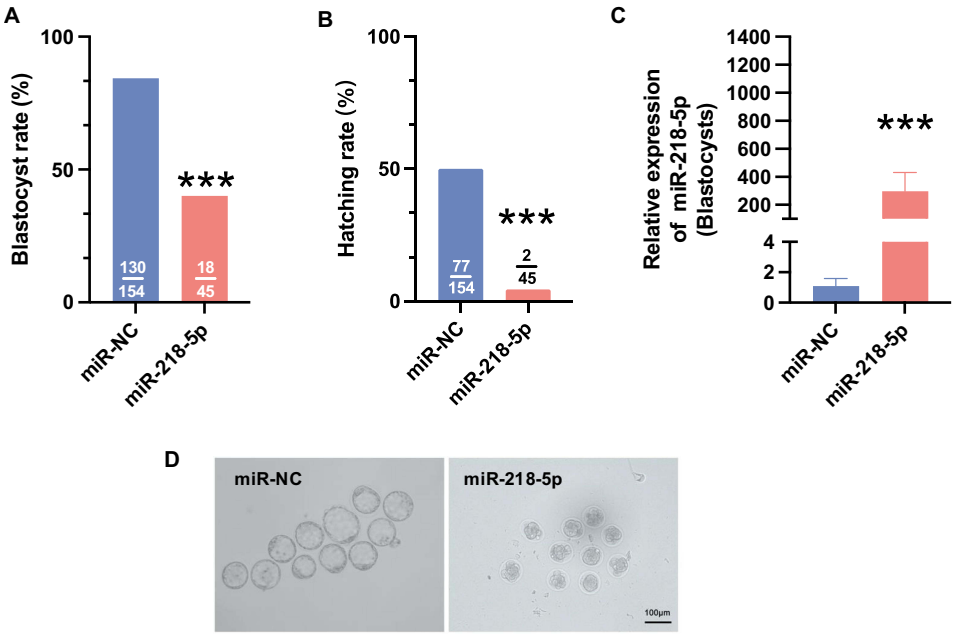

Figure 1 Impaired mouse blastocyst formation following miR-218-5p treatment. (**A** and **B**) Blastocyst rate and hatching rate of the embryos in each group, numbers of initial 4-cell-stage embryo at E2.0 and the number of blastocyst and hatching embryos were shown as denominator and numerator, respectively. (**C**) Relative expression of miRNAs in the blastocyst post-agomir treatment of miRNAs. (**D**) Bright field of mice embryos after miR-218-5p treatment. ***date significant difference between the miR-218-5p treatment group and the negative control group ($P < 0.001$).

https://doi.org/10.2147/IJN.S508491

Table 2 The Embryo Development Rate After miR-218-5p Treatment

	miR-NC	miR-218-5p
E2.5		
No. Total embryos	149	130
No. 8 cell (rate, %)	99 (66.4)	57 (43.9)
E3.25		
No. Total embryos	156	173
No. Morula (rate, %)	133 (85.3)	104 (60.1)
E4.5		
No. Total embryos	37	86
No. Collapsed embryos (rate, %)	7 (19.0)	12 (13.4)
No. Blastocyst (rate, %)	27 (73.0)	29 (33.7)
No. Morula (rate, %)	3 (8.1)	45 (52.3)
E5.5		
No. Total embryos	59	73
No. Collapsed embryos (rate, %)	8 (13.6)	26 (35.6)
No. Blastocyst (rate, %)	48 (81.4)	16 (21.9)
No. Morula (rate, %)	3 (5.0)	31 (42.5)

embryos from E2.5 to E4.5, and embryos were arrested at the morula stage with the failure of blastocyte formation during prolonged cultivation until E5.5. Consistent with the observed embryo quality, the total cell number (TCN) was significantly lower in miR-218-5p group compared to miR-NC group in both morula (E3.25) and expanded blastocyst (E4.5), respectively (Figure 2B–D). The interruption of blastocyst formation at E4.5 caused by miR-218-5p agomir was present in a dose-dependent manner (Figure 2E–G). Additionally, there was a reduction in EdU-positive blastomeres (Supplemental Figure 3).

miR-218-5p Impaired the Lineage Specification of the Arrested Mouse Morula

Transcriptional changes during the compaction phase determine the fate of the blastocyst.[44,45] To explore the mechanism behind morula arrest in miR-218-5p embryos, we compared the transcriptomes of compacted morula in miR-218-5p and NC groups at E3.25. Total 445, and 474 genes were identified as up or down-regulated, respectively, in the miR-218-5p group morula (Figure 3A and Supplemental Table 1). The KEGG analysis (Figure 3B and Supplemental Table 2) of the differential transcripts in miR-218-5p morula were produced. Heat map of the DEGs was shown in Figure 3C. As shown in Figure 3D–F and Supplemental Table 3, the Gene Ontology (GO) analysis of DEGs between miR-218-5p and miR-NC morula were produced in Cellular Component (CC), Molecular Function (MF), and Biological Process (BP), respectively. Interestingly, KEGG analysis revealed enrichment of gene sets in the Hippo signaling pathway, a crucial regulator in cell fate decisions prior to the blastocyst formation, particularly in the segregation of the trophectoderm (TE) and inner cell mass (ICM).[46,47]

We endeavored to investigate the underlying biological processes associated with arrested development of the morula in the miR-218-5p group. KEGG analysis suggested that the impaired blastocyte formation observed in RIF-EVs encapsulated-miR-218-5p could be due to an atypical differentiation of ICM and TE. The morula presents as the initiated specification of TE and ICM lineage.[48] We first detected the mRNA expression of key genes for lineage specification. As shown in Figure 4A, the specific ICM marker genes Sox2[49] and TE-related genes Tead4, Cdx2, and Yap1[50] were decreased in miR-218-5p morula. These RT-qPCR results suggested that the compromised differentiation may have led to the arrest of embryo development, which is consistent with our RNA-seq findings. However, we failed to detect the differential state in apoptosis activation, mitochondrial membrane potential, and Reactive Oxygen Species (ROS) between the miR-218-5p and miR-NC embryos (Supplemental Figure 4). We further analyzed the miR-218-5p and miR-NC morula by immunofluorescence staining of the Cdx2, which is the key transcription factor for the TE differentiation in mammalian.[51,52] We found that the Cdx2 nuclei positive morula in miR-218-5p group (35.2%) were

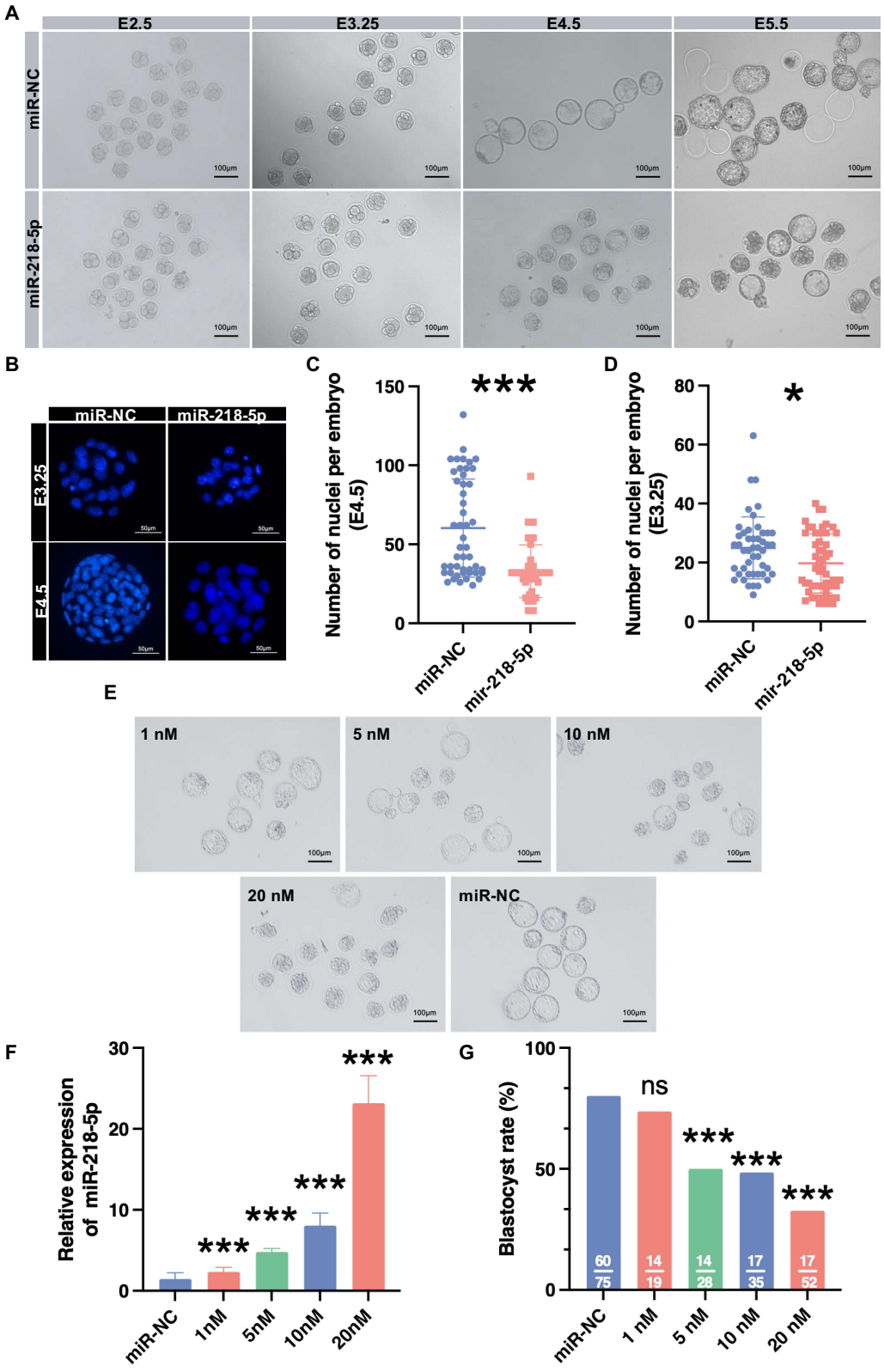

Figure 2 miR-218-5p induces arrest of pro-implantation embryos at the morula stage (**A**) Bright field images post-treatment with either miR-NC or miR-218-5p agomir at various developmental stages. (**B**) Representative confocal microscopy images showing DAPI staining of morulae or blastocysts (**C** and **D**) Total cell number of embryos at E 3.25 and E4.5, respectively. (**E**) Bright field images of embryos at E4.5 after different concentrations of miR-218-5p treatment. (**F** and **G**) Relative expression of miRNAs in the blastocyst and blastocyte rate after different concentrations of miR-218-5p treatment. ***date significant difference between the agomir treatment group and the negative control group ($P < 0.001$); *$P < 0.05$; ns, no significant difference. The scar bar is 100 μm in bright field images and 50 μm in DAPI staining images.

https://doi.org/10.2147/IJN.S508491

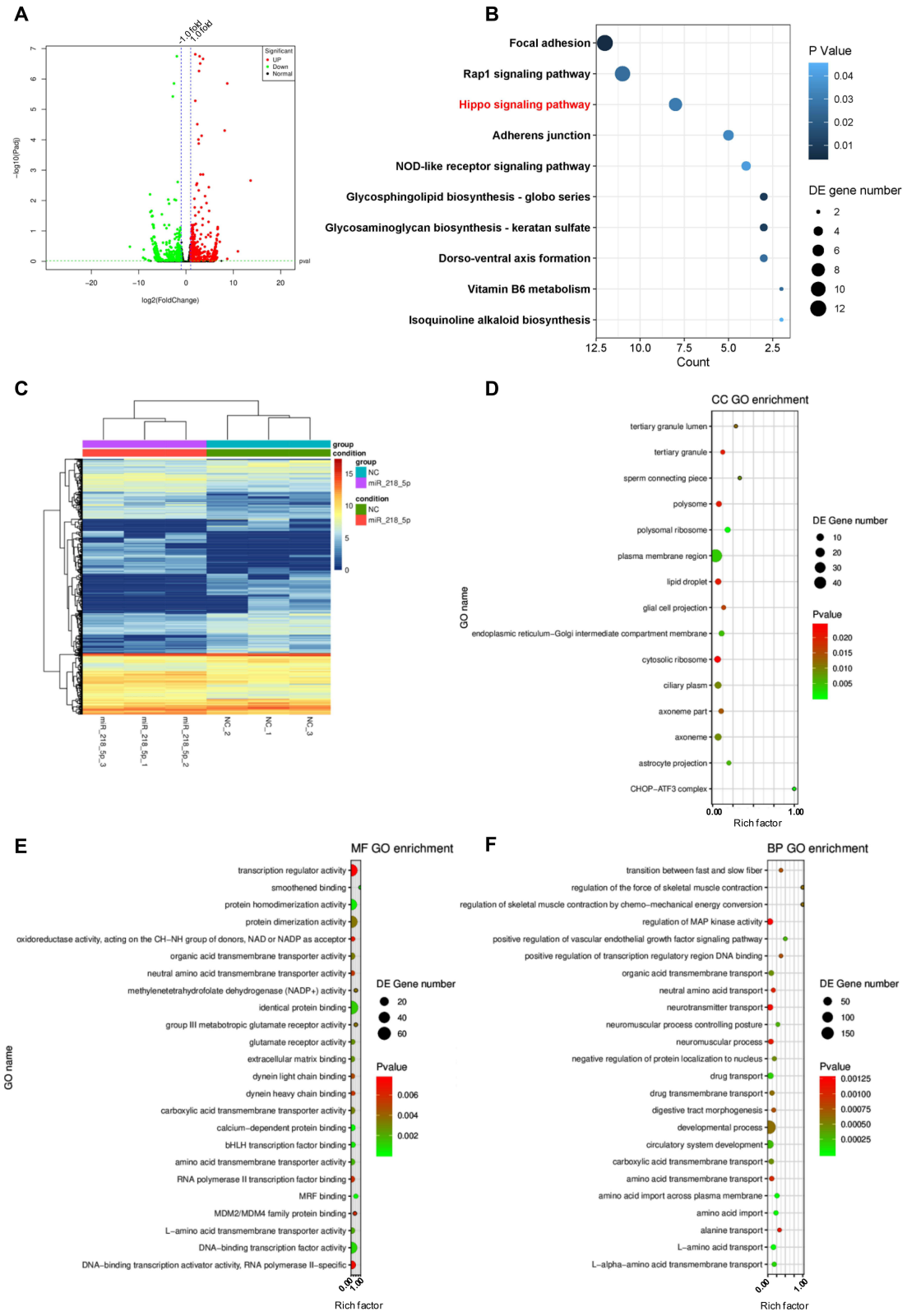

Figure 3 The differential transcriptomics of mouse morula between miR-218-5p and miR-NC groups. (**A**) Volcano plot of differentially expressed genes following miR-218-5p agomir treatment in morula. Red and green dots represented up-regulated and down-regulated genes, respectively. (**B**) KEGG analysis of differentially expressed genes, with dot size indicating the number of genes included and color representing *P*-value significance. The red text is the highlight of the Hippo signaling pathway. (**C**) Heat map of the DEGs. (**D**–**F**) Bubble plots of gene ontology (GO) categories: Cellular Components (CC), Biological Process (BP), Molecular Function (MF). The size of the dots represents the number of included genes, and the color of the dots indicates the *P* value.

Abbreviations: DEGs, differentially expressed genes; KEGG, Kyoto Encyclopedia of Genes and Genomes.

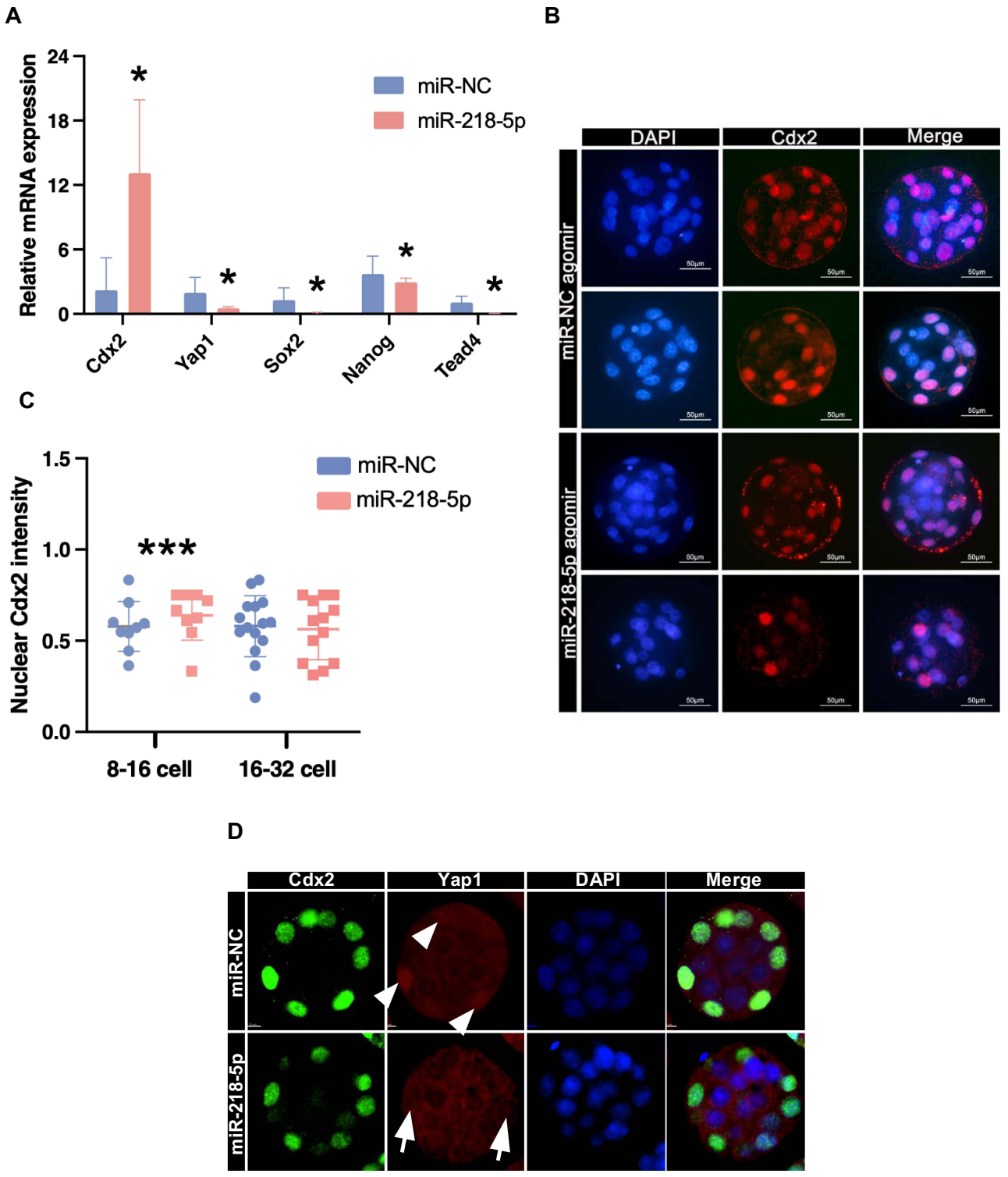

Figure 4 miR-218-5p impaired the lineage specification in the arrested morula. (**A**) Relative mRNA expression of lineage specification-related genes in morula treated with miR-218-5p agomir. (**B**) Representative confocal microscopy images displaying Cdx2 expression in morula treated with either miR-NC or miR-218-5p. (**C**) Cdx2 nuclear intensity in miR-NC or miR-218-5p groups at 8–16 and 16–32 cell stages, respectively. (**D**) Localization of Cdx2 (green) and Yap1 (red) and nuclei (blue) in miR-NC or miR-218-5p treated morula. Yap1 presence in the Cdx2 positive nuclei is indicated by white arrows, and absence is indicated by white arrowheads. *$P < 0.5$; ***$P < 0.001$; Scale bars, 50 μm.

significantly lower than the miR-NC groups (60.8%, $P < 0.001$) at the 8–16-cell stage, which is the initiated asymmetric diversion of the embryos into ICM and TE lineages[53] (Figure 4B and C). As a key TF in the Hippo signaling pathway in cell fate determination, Yap1 is located in the nuclei of the outer cell of the morula in both mice and human.[54,55] In the

https://doi.org/10.2147/IJN.S508491

miR-218-5p group, we observed a disappearance of Yap1 nuclear signals in Cdx2 positive blastomeres, while in the control group, overlapping nuclear expression of Cdx2 and Yap1 was evident in the outer cell layer of the morula (Figure 4D). Hence, the expression of lineage specification-related Cdx2 and the distribution of Yap1 protein were disrupted by the miR-218-5p agmoir treatment.

Engineered Extracellular Vesicles Encapsulating Anti-miR-218-5p Counteracted the Detrimental Effects Caused by miR-218-5p

MiR-218-5p disrupts blastocyte cavity formation and is a critical molecule encapsulated in the RIF-EVs. Consequently, we explored whether it is feasible to counteract these adverse effects within the embryo development microenvironment. Therefore, we conducted engineered EVs (E-EVs) encapsulated with anti-miR-218-5p. The common methods of the exogenous RNA encapsulated into EVs include lipofection,[56,57] sonication,[58] chemical transfection,[57] electroporation,[59,60] and the peptide-based method.[40] The peptide-based method using the cell-penetrating peptide offers an efficacious and straightforward promising approach to load the RNAs into EVs. Thus, we loaded anti-miR-218-5p via a cell-peptide technique in utilizing Human Umbilical Cord Mesenchymal Stem Cells (HUMSC)-derived EVs, which minimally affect embryo development.[61,62] The identification of HUMSCs was analyzed by flow cytometry (Supplemental Figure 5). The characterization of the EVs and E-EVs was firstly identified by NTA, Western Blot, and TEM. As shown in Figure 5A–C, the mean sizes of the EVs (129.5nm) and

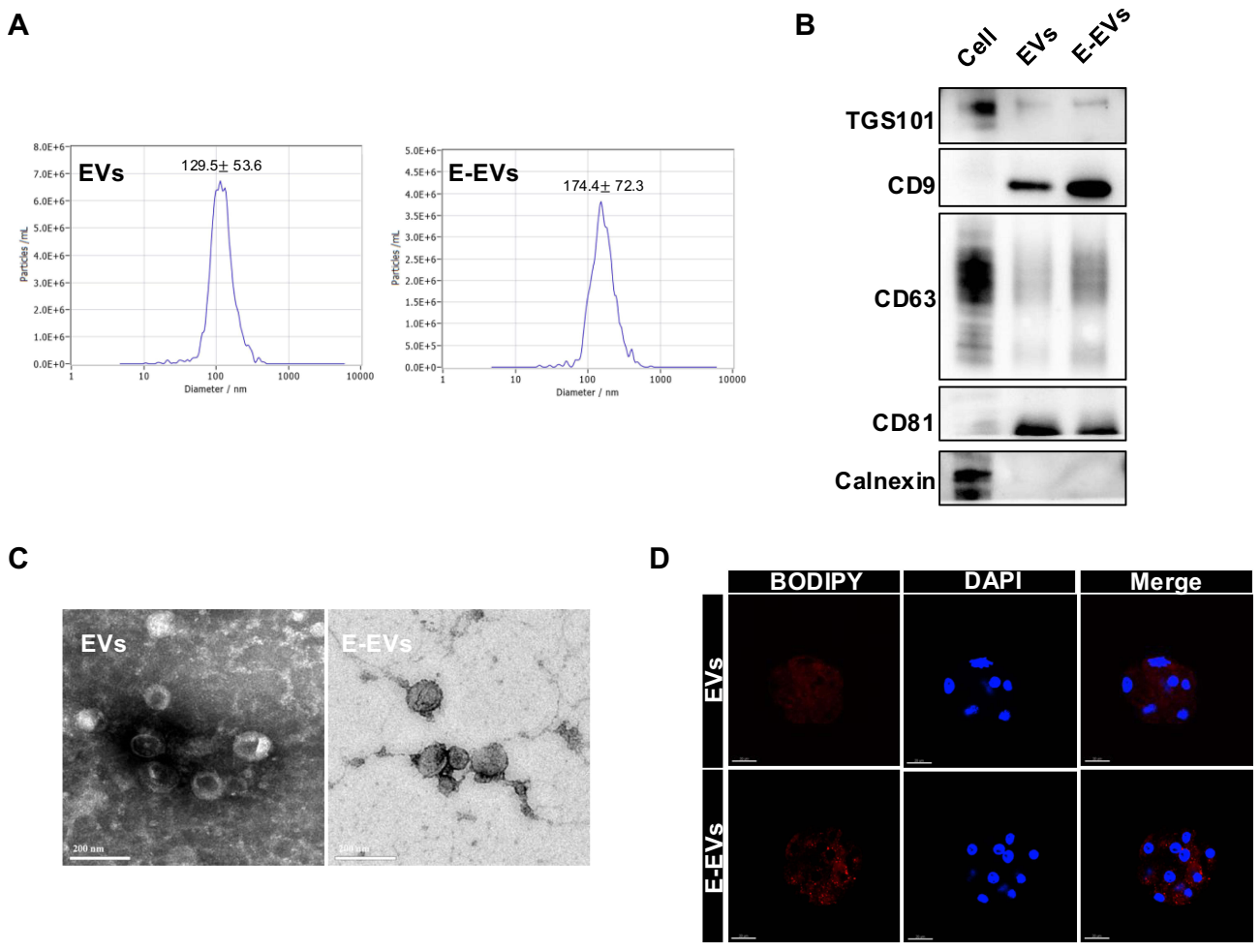

Figure 5 Characters and the internalization of extracellular vesicles and engineered extracellular vesicles. (**A**) Size and distribution of EVs and E-EVs as detected by Nanoparticle Tracking Analysis (NTA). (**B**) Western blotting analysis confirming the expression of classic EV protein markers in EVs and E-EVs. (**C**) Morphology of EVs and E-EVs as observed via Transmission Electron Microscopy (TEM). Scale bars set to 200 nm. (**D**) Representative confocal images of mice morula co-cultured with BODIPY TR ceramide (red) labeled EVs and E-EVs, with blastomere nuclei stained by DAPI (blue). Scale bars, 50 μm.

Abbreviations: NTA, nanoparticle tracking analysis; TEM, transmission electron microscopy; DAPI, 4′,6-diamidino-2-phenylindole.

E-EVs (174.4nm) particles were all under 200 nm, the EVs markers were presented at both EVs and E-EVs, the Calnexin was presented in whole-cell lysate only. The double layer of the particles was clear in both EVs and E-EVs, which was consistent with the typical EVs.[63] As shown in Figure 5D, the fluorescently labeled EVs and E-EVs were efficiently internalized by the embryo. The loading efficiency was shown in Supplemental Figure 6. We next pre-treated embryos with the same concentration of EVs or E-EVs (2×10^{10} particles/mL), or 3 nM anti-miR-218-5p for 10 h, which is the same concentration as the engineered EVs packaging. Followed by the miR-218-5p agomir treatment, the embryo development was monitored until E4.5. As shown in Figure 6A, HUMSC-derived EVs alone did not affect blastocyst formation nor mitigate the adverse effects of miR-218-5p agomir. However, E-EVs significantly alleviated the decrease in blastocyte rate induced by miR-218-5p agomir. The TCN of the blastocytes increased in the E-EVs groups, and there were no significant differences in TCN between the anti-miR-218-5p and miR-218-5p agomir groups (Figure 6B). The representative images of the TCN were shown in Figure 6C, bright field images were shown in Figure 6D.

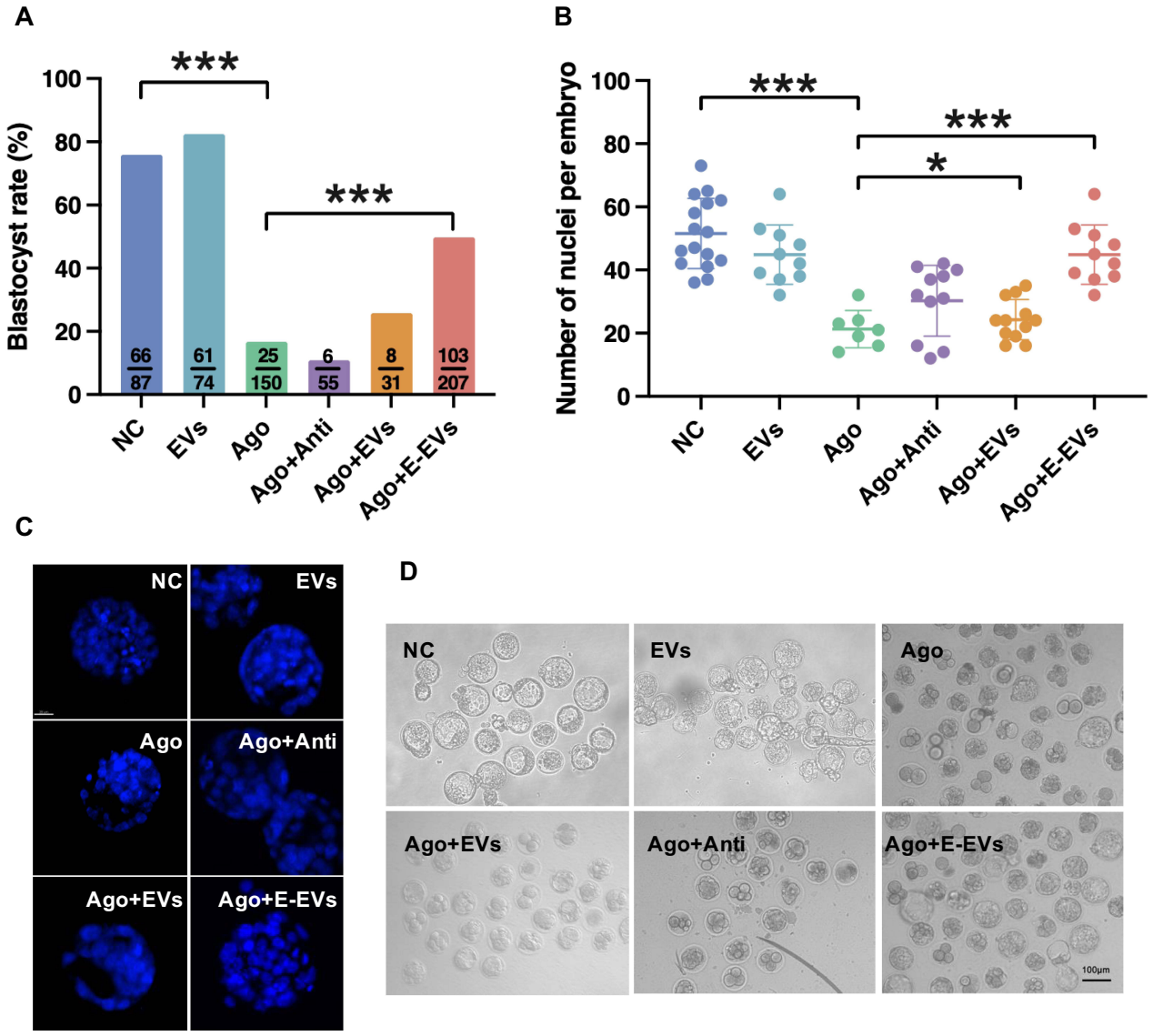

Figure 6 Effects of engineered extracellular vesicles on mouse preimplantation embryo development. (**A**) The blastocyte rate of the mice embryo, numbers of the initial 4-cell-stage embryo at E2.0 and the number of blastocysts were shown as denominator and numerator. (**B**) Total cell number (TCN) of the embryo at E4.5. (**C**) Representative confocal images of blastomere nuclei DAPI staining, Scale bars set to 50 μm. (**D**) Bright fried images of the embryo at E4.5. Ago, miR-218-5p agomir; Ago+Anti, miR-218-5p agomir and anti-miR-218-5p group; Ago+EVs, miR-218-5p agomir and small extracellular vesicles group; Ago+E-EVs, miR-218-5p agomir and engineered small extracellular vesicles group. *$P < 0.5$; ***$P < 0.001$.
Abbreviations: NC, negative control; DAPI, 4′,6-diamidino-2-phenylindole.

https://doi.org/10.2147/IJN.S508491

Discussion

RIF is a puzzling condition with a complex etiology that affects couples undergoing ART.[4] In the present study, we uncovered that miR-218-5p was the effective cargo of the RIF-EVs, which induced the embryo arrested at the morula stage with an apparent delay of compaction. The aberrant segregation of cell lineages contributed to this phenotype on account of the changes in complete transcriptomes and decreased expression of Cdx2 before the 16-cell stage in miR-218-5p treated embryos. Interestingly, we discovered that Yap1, a key transcription factor in the Hippo signaling pathway,[55,64] lost its co-location with Cdx2 in the outer cell of the morula due to exogenous miR-218-5p. To counteract the detrimental impact of RIF-EVs-miR-218-5p, we conducted the E-EVs encapsulated with anti-miRNAs in specifically targeting miR-218-5p. Upon co-culturing the E-EVs with mouse embryos, these E-EVs effectively diminished the RIF-EVs-miR-218-5p-induced disruption in embryonic development within the microenvironment, indicating that they could be a promising nanotherapeutic avenue for treating the RIF embryo injury.

Maternal reproductive tract EVs are crucial for mother-fetus communication and embryonic development.[10,65–68] Significant differences in gene patterns exist between endometrial and intrauterine fluid EVs of RIF patients and fertile women,[11,23] however, most of them are bioinformatics studies and focus just on transcriptomic,[24,69–73] lacking in-depth molecular mechanism investigations. We identified that miR-218-5p interrupted the expansion of blastocoels which may be considered as the functional molecular in RIF-EVs. Previous studies have suggested that miR-218-5p is correlated with bovine ICM formation based on bioinformatics analyses only.[34] Our findings offer the initial evidence suggesting that miR-218-5p may have detrimental effects on mouse embryo development.

Given that miR-218-5p is the most highly expressed functional miRNA in RIF-EVs, we were particularly interested in understanding the mechanisms underlying miR-218-5p-induced embryonic diapause. We observed miR-218-5p-treated mouse embryos from E2.5 to E5.5. The 8-cell rate, morula rate, and blastocyst rate all decreased in the miR-218-5p group, indicating a significant developmental delay caused by miR-218-5p. Most notably, even when we extended the observation time to the post-hatching stage at E5.5, the blastocyst rate in the miR-218-5p group did not increase; instead, the quantity of collapsed embryos rose. These observations led us to deduce that miR-218-5p specifically arrested mouse embryos at the morula stage, rather than merely causing a developmental delay. The morula stage is the crucial time in determining the fate of the blastomeres when they acquire the first signs of polarity,[74,75] followed by the re-localization of cadherin–catenin complexes accompanied by the intercellular adhesion increases, then, blastomeres gradually compaction.[76,77] The compaction process in mammalian embryos is remarkably intricate, marked by a sequence of crucial molecular activities.[31,78,79] We discovered that the DEGs in miR-218-5p arrested morula were enriched in lineage speciation-related genes. Interestingly, we found that the Cdx2 protein expression was significantly lower in the miR-218-5p group during the 8–16-cell stage, while not the 16–32 cell stage. The blastomere undergoes first asymmetric divisions at the 8–16-cell stage (fourth cleavage), and this process is highly programmed, rather than random. The inner cell and outer cell of the blastomere were distinguished, which exclusively develop into ICM and TE of the embryos, respectively.[80,81] The Cdx2 distribution is polarized in the apical domains of the outer blastomeres, which are upon differentiative divisions at 8–16-cell in a specific manner.[82] The natural embryo development tracking in individual cells indicated that the highly expressed Cdx2 blastomere at the 8-cell stage contributed to TE eventually.[83] In our observation, the expression of Cdx2 was decreased by RIF-EVs-miR-218-5p at the 8–16-cell stage, which inspired us that the initial asymmetric divisions may be interrupted by miR-218-5p. When the embryo reaches to 16–32 cell stage, the fifth cleavage will be efficacious on the outer cell,[83,84] and the differential expression of the Cdx2 becomes undetectable in the whole morula. The successful formation of the blastocyst relies on higher Cdx2 cells preferentially contributing to the TE, while lower Cdx2 level cells are predisposed to the ICM. A Cdx2-null trophectoderm is incapable of sustaining its polarizing structure and forming to blastocyst.[85] This observation aligns with our findings, where the reduction of Cdx2 at the fourth cleavage due to miR-218-5p in company with the blastocoel formation failure. Yap1, one of the key TFs in the Hippo signaling pathway,[86] is restricted to outer cell nuclei and binding with Tead4 to initiate Cdx2 expression in compaction.[87] In naturally normal mouse morulae, nuclear Yap1 and Cdx2 are found concurrently in the nuclei of outer cells, exclusively.[46] We found that the miR-218-5p treatment losing the colocalization of the Cdx2 in the morula outer cells. This is consistent with our KEGG analysis, which shows an enrichment of DEGs in the Hippo signaling pathway in

miR-218-5p affected morulae. These results imply that the miR-218-5p treatment triggers a disruption in the Yap1-driven Hippo signaling pathway.

The application of EVs in reproduction medicine is a highly encouraging and auspicious approach. It has been found that EVs derived from endometrial stromal cells can promote mouse embryo cleavage and blastocyst formation, and these EVs contain numerous proteins related to embryonic development such as transferrin, vinculin, fibronectin, matrix metalloproteinase-2 (MMP2), and E-cadherin.[88] EVs from pig oviducts promote embryo development and alter the transcriptome information of embryos, and similar results have been confirmed in the in vitro culture of cow and rabbit embryos.[89–91] We used artificially synthesized and loaded EVs carrying anti-miRNAs to treat mouse embryos. These E-EVs were taken up by mouse embryos and reversed the adverse effects of RIF-EVs on embryonic development. Engineered EVs have a wide range of biological applications, and their therapeutic effects on diseases have been increasingly recognized and verified.[92,93] It has been found that loading miRNA antisense chains into EVs derived from bone marrow mesenchymal stem cells not only enhances nucleic acid uptake efficiency but also exhibits a significant therapeutic effect on mouse muscle atrophy. Similarly, EVs derived from mesenchymal stem cells after obtaining miR-582 loading can interfere with the metastasis of melanoma. EVs loaded with miR-675 can promote the reperfusion of ischemic limbs.[94–96] The therapeutic potential of engineered EVs in treating various diseases is increasingly being acknowledged and validated. We constructed the efficacious E-EVs in reversing the effect of miR-218-5p on mouse embryo development. Those results made a great convenient tool for researchers to study embryonic development and even inspired the therapeutic method in RIF. EVs themselves are less harmful to the mental state of the embryo compared to other methods, as they do not directly alter the embryo's genetic code or induce any toxic effects. Also, the E-EVs provide a protective environment for the anti-miRNA, preventing it from being degraded or eliminated. Nevertheless, a limitation of our research is that it was solely conducted on mice. Subsequent investigations in more advanced animal models and eventual clinical trials involving humans will be imperative to comprehensively establish both efficacy and safety, taking into account long-term safety implications and potential side effects. Overall, the use of E-EVs in embryonic development shows great promise in improving embryo quality and increasing the chances of successful implantation, while also providing a safe and convenient tool for researchers to study embryonic development.

Conclusion

This study provides critical insights into the adverse effects of miR-218-5p on pre-implantation embryo development in mice. Furthermore, we unveiled the potential of E-EVs containing anti-miR-218-5p as a promising strategy for mitigating these detrimental effects. This research not only expands our understanding of the molecular mechanisms underlying reproductive disorders but also paves the way for the development of innovative strategies to enhance embryo quality.

Abbreviations

RIF, Recurrent implantation failure; EVs, extracellular vesicles; TE, trophectoderm; ICM, inner cell mass; ART, assisted reproductive technology; E-EVs, engineered extracellular vesicles; ICR, Institute of Cancer Research; PMSG, pregnant mare's serum gonadotropin; GO, Gene ontology; KEGG, Kyoto Encyclopedia of Genes and Genomes; PFA, paraformaldehyde; NTA, Nanoparticle tracking analysis; TEM, Transmission electron microscopy; TCN, total cell number; HUMSC, Human Umbilical Cord Mesenchymal Stem Cells; DEGs, differentially expressed genes.

Data and Materials Availability

All data needed to evaluate the conclusions in this paper are present in the paper and/or the Supplementary Materials. The authors confirm that the data supporting the findings of this study are available within the article and its supplementary materials.

Ethics Approval

All animal experiments were approved by the Medical Ethics Committee of Tongji Medical College, Huazhong University of Science and Technology (2022S067).

Acknowledgments

L.C. and M.L contributed equally to this work. L.C. would thank Shitong Lin for his kindly support on language edit, and Shiyu Li for his kindly help.

Funding

This work was supported by the Foundation of Tongji Hospital (No. 2020JZKT469).

Disclosure

The authors declare no conflict of interest.

References

1. Koot YEM, Hviid Saxtorph M, Goddijn M, et al. What is the prognosis for a live birth after unexplained recurrent implantation failure following IVF/ICSI? *Hum Reprod*. 2019;34:2044–2052. doi:10.1093/humrep/dez120
2. Shaulov T, Sierra S, Sylvestre C. Recurrent implantation failure in IVF: a Canadian Fertility and Andrology Society Clinical Practice Guideline. *Reprod Biomed Online*. 2020;41:819–833. doi:10.1016/j.rbmo.2020.08.007
3. Thornhill AR, deDie-Smulders CE, Geraedts JP, et al. ESHRE PGD Consortium 'Best practice guidelines for clinical preimplantation genetic diagnosis (PGD) and preimplantation genetic screening (PGS)'. *Hum Reprod*. 2005;20:35–48. doi:10.1093/humrep/deh579
4. Cimadomo D, Craciunas L, Vermeulen N, Vomstein K, Toth B. Definition, diagnostic and therapeutic options in recurrent implantation failure: an international survey of clinicians and embryologists. *Hum Reprod*. 2021;36:305–317. doi:10.1093/humrep/deaa317
5. Franasiak JM, Alecsandru D, Forman EJ, et al. A review of the pathophysiology of recurrent implantation failure. *Fertil Steril*. 2021;116:1436–1448. doi:10.1016/j.fertnstert.2021.09.014
6. Ata B, Kalafat E, Somigliana E. A new definition of recurrent implantation failure on the basis of anticipated blastocyst aneuploidy rates across female age. *Fertil Steril*. 2021;116:1320–1327. doi:10.1016/j.fertnstert.2021.06.045
7. Kliman HJ, Frankfurter D. Clinical approach to recurrent implantation failure: evidence-based evaluation of the endometrium. *Fertil Steril*. 2019;111:618–628. doi:10.1016/j.fertnstert.2019.02.011
8. Simon C, Greening DW, Bolumar D, et al. Extracellular vesicles in human reproduction in health and disease. *Endocr Rev*. 2018;39:292–332. doi:10.1210/er.2017-00229
9. Kalluri R, LeBleu VS. The biology, function, and biomedical applications of exosomes. *Science*. 2020;367. doi:10.1126/science.aau6977
10. Bridi A, Perecin F, Silveira JCD. Extracellular vesicles mediated early embryo-maternal interactions. *Int J mol Sci*. 2020;21:1163. doi:10.3390/ijms21031163
11. Li T, Greenblatt EM, Shin ME, Brown TJ, Chan C. Cargo small non-coding RNAs of extracellular vesicles isolated from uterine fluid associate with endometrial receptivity and implantation success. *Fertil Steril*. 2021;115:1327–1336. doi:10.1016/j.fertnstert.2020.10.046
12. Rai A, Poh QH, Fatmous M, et al. Proteomic profiling of human uterine extracellular vesicles reveal dynamic regulation of key players of embryo implantation and fertility during menstrual cycle. *Proteomics*. 2021;21:e2000211. doi:10.1002/pmic.202000211
13. Cao D, Liu Y, Cheng Y, et al. Time-series single-cell transcriptomic profiling of luteal-phase endometrium uncovers dynamic characteristics and its dysregulation in recurrent implantation failures. *Nat Commun*. 2025;16:137. doi:10.1038/s41467-024-55419-z
14. Noyes RW, Hertig AT, Rock J. Reprint of: dating the endometrial biopsy. *Fertil Steril*. 2019;112:e93–e115. doi:10.1016/j.fertnstert.2019.08.079
15. Liu C, Yao W, Yao J, et al. Endometrial extracellular vesicles from women with recurrent implantation failure attenuate the growth and invasion of embryos. *Fertil Steril*. 2020;114:416–425. doi:10.1016/j.fertnstert.2020.04.005
16. Ng YH, Rome S, Jalabert A, et al. Endometrial exosomes/microvesicles in the uterine microenvironment: a new paradigm for embryo-endometrial cross talk at implantation. *PLoS One*. 2013;8:e58502. doi:10.1371/journal.pone.0058502
17. Greening DW, Nguyen HP, Elgass K, Simpson RJ, Salamonsen LA. Human endometrial exosomes contain hormone-specific cargo modulating trophoblast adhesive capacity: insights into endometrial-embryo interactions. *Biol Reprod*. 2016;94:38. doi:10.1095/biolreprod.115.134890
18. Liu C, Wang M, Zhang H, Sui C. Altered microRNA profiles of extracellular vesicles secreted by endometrial cells from women with recurrent implantation failure. *Reprod Sci*. 2021;28:1945–1955.
19. Bartel DP. MicroRNAs: target recognition and regulatory functions. *Cell*. 2009;136:215–233. doi:10.1016/j.cell.2009.01.002
20. Garcia-Martin R, Wang G, Brandão BB, et al. MicroRNA sequence codes for small extracellular vesicle release and cellular retention. *Nature*. 2022;601:446–451. doi:10.1038/s41586-021-04234-3
21. Segura-Benítez M, Carbajo-García MC, Quiñonero A, et al. Endometrial extracellular vesicles regulate processes related to embryo development and implantation in human blastocysts. *Hum Reprod*. 2025;40:56–68. doi:10.1093/humrep/deae256
22. Qin X, Hu K-L, Li Q, et al. In situ sprayed hydrogel delivers extracellular vesicles derived from human endometrial organoids for uterine function preservation and fertility restoration. *Adv Healthc Mater*. 2025;14:e2403604. doi:10.1002/adhm.202403604
23. Koler M, Achache H, Tsafrir A, et al. Disrupted gene pattern in patients with repeated in vitro fertilization (IVF) failure. *Hum Reprod*. 2009;24:2541–2548. doi:10.1093/humrep/dep193
24. von Grothusen C, Frisendahl C, Modhukur V, et al. Uterine fluid microRNAs are dysregulated in women with recurrent implantation failure. *Hum Reprod*. 2022;37:734–746. doi:10.1093/humrep/deac019
25. Yang Y, Bai W, Zhang L, et al. Determination of microRNAs in mouse preimplantation embryos by microarray. *Dev Dyn*. 2008;237:2315–2327. doi:10.1002/dvdy.21666
26. Suh N, Baehner L, Moltzahn F, et al. MicroRNA function is globally suppressed in mouse oocytes and early embryos. *Curr Biol*. 2010;20:271–277. doi:10.1016/j.cub.2009.12.044

27. Misirlioglu M, Page GP, Sagirkaya H, et al. Dynamics of global transcriptome in bovine matured oocytes and preimplantation embryos. *Proc Natl Acad Sci U S A*. 2006;103:18905–18910. doi:10.1073/pnas.0608247103
28. Tang F, Kaneda M, O'Carroll D, et al. Maternal microRNAs are essential for mouse zygotic development. *Genes Dev*. 2007;21:644–648. doi:10.1101/gad.418707
29. Salilew-Wondim D, Gebremedhn S, Hoelker M, et al. The role of MicroRNAs in mammalian fertility: from gametogenesis to embryo implantation. *Int J Mol Sci*. 2020;21:585. doi:10.3390/ijms21020585
30. Bushati N, Stark A, Brennecke J, Cohen SM. Temporal reciprocity of miRNAs and their targets during the maternal-to-zygotic transition in Drosophila. *Curr Biol*. 2008;18:501–506. doi:10.1016/j.cub.2008.02.081
31. Li L, Zheng P, Dean J. Maternal control of early mouse development. *Development*. 2010;137:859–870. doi:10.1242/dev.039487
32. Tripurani SK, Wee G, Lee K-B, et al. MicroRNA-212 post-transcriptionally regulates oocyte-specific basic-helix-loop-helix transcription factor, factor in the germline alpha (FIGLA), during bovine early embryogenesis. *PLoS One*. 2013;8:e76114. doi:10.1371/journal.pone.0076114
33. Sinha PB, Tesfaye D, Rings F, et al. MicroRNA-130b is involved in bovine granulosa and cumulus cells function, oocyte maturation and blastocyst formation. *J Ovarian Res*. 2017;10:37. doi:10.1186/s13048-017-0336-1
34. Goossens K, Mestdagh P, Lefever S, et al. Regulatory microRNA network identification in bovine blastocyst development. *Stem Cells Dev*. 2013;22:1907–1920. doi:10.1089/scd.2012.0708
35. Tan Q, Shi S, Liang J, et al. MicroRNAs in small extracellular vesicles indicate successful embryo implantation during early pregnancy. *Cells*. 2020;9:645. doi:10.3390/cells9030645
36. de Abreu RC, Ramos CV, Becher C, et al. Exogenous loading of miRNAs into small extracellular vesicles. *J Extracell Vesicles*. 2021;10:e12111. doi:10.1002/jev2.12111
37. Picelli S, Björklund ÅK, Faridani OR, et al. Smart-seq2 for sensitive full-length transcriptome profiling in single cells. *Nature Methods*. 2013;10:1096–1098. doi:10.1038/nmeth.2639
38. Xie Y, Sun Y, Liu Y, et al. Targeted delivery of RGD-CD146(+)CD271(+) human umbilical cord mesenchymal stem cell-derived exosomes promotes blood-spinal cord barrier repair after spinal cord injury. *ACS Nano*. 2023;17:18008–18024. doi:10.1021/acsnano.3c04423
39. Lobb RJ, Becker M, Wen Wen S, et al. Optimized exosome isolation protocol for cell culture supernatant and human plasma. *J Extracell Vesicles*. 2015;4:27031. doi:10.3402/jev.v4.27031
40. Hade MD, Suire CN, Suo Z. An effective peptide-based platform for efficient exosomal loading and cellular delivery of a microRNA. *ACS Appl Mater Interfaces*. 2023;15:3851–3866. doi:10.1021/acsami.2c20728
41. Takada S, Berezikov E, Yamashita Y, et al. Mouse microRNA profiles determined with a new and sensitive cloning method. *Nucleic Acids Res*. 2006;34:e115. doi:10.1093/nar/gkl653
42. Viswanathan SR, Mermel CH, Lu J, et al. microRNA expression during trophectoderm specification. *PLoS One*. 2009;4:e6143. doi:10.1371/journal.pone.0006143
43. Ohnishi Y, Totoki Y, Toyoda A, et al. Small RNA class transition from siRNA/piRNA to miRNA during pre-implantation mouse development. *Nucleic Acids Res*. 2010;38:5141–5151. doi:10.1093/nar/gkq229
44. Xue Z, Huang K, Cai C, et al. Genetic programs in human and mouse early embryos revealed by single-cell RNA sequencing. *Nature*. 2013;500:593–597. doi:10.1038/nature12364
45. Vassena R, Boué S, González-Roca E, et al. Waves of early transcriptional activation and pluripotency program initiation during human preimplantation development. *Development*. 2011;138:3699–3709. doi:10.1242/dev.064741
46. Nishioka N, Inoue KI, Adachi K, et al. The Hippo signaling pathway components Lats and Yap pattern Tead4 activity to distinguish mouse trophectoderm from inner cell mass. *Dev Cell*. 2009;16:398–410. doi:10.1016/j.devcel.2009.02.003
47. Frum T, Murphy TM, Ralston A. HIPPO signaling resolves embryonic cell fate conflicts during establishment of pluripotency in vivo. *Elife*. 2018;7. doi:10.7554/eLife.42298
48. Johnson MH, Ziomek CA. The foundation of two distinct cell lineages within the mouse morula. *Cell*. 1981;24:71–80. doi:10.1016/0092-8674(81)90502-X
49. Li L, Lai F, Hu X, et al. Multifaceted SOX2-chromatin interaction underpins pluripotency progression in early embryos. *Science*. 2023;382:eadi5516. doi:10.1126/science.adi5516
50. Stamatiadis P, Cosemans G, Boel A, et al. TEAD4 regulates trophectoderm differentiation upstream of CDX2 in a GATA3-independent manner in the human preimplantation embryo. *Hum Reprod*. 2022;37:1760–1773. doi:10.1093/humrep/deac138
51. Niwa H, Toyooka Y, Shimosato D, et al. Interaction between Oct3/4 and Cdx2 determines trophectoderm differentiation. *Cell*. 2005;123:917–929. doi:10.1016/j.cell.2005.08.040
52. Jedrusik A, Parfitt D-E, Guo G, et al. Role of Cdx2 and cell polarity in cell allocation and specification of trophectoderm and inner cell mass in the mouse embryo. *Genes Dev*. 2008;22:2692–2706. doi:10.1101/gad.486108
53. Zernicka-Goetz M. First cell fate decisions and spatial patterning in the early mouse embryo. *Semin Cell Dev Biol*. 2004;15:563–572. doi:10.1016/j.semcdb.2004.04.004
54. Hirate Y, Cockburn K, Rossant J, Sasaki H. Tead4 is constitutively nuclear, while nuclear vs. cytoplasmic Yap distribution is regulated in preimplantation mouse embryos. *Proc Natl Acad Sci U S A*. 2012;109:E3389–3390;authorreplyE3391–3382.
55. Gerri C, McCarthy A, Alanis-Lobato G, et al. Initiation of a conserved trophectoderm program in human, cow and mouse embryos. *Nature*. 2020;587:443–447. doi:10.1038/s41586-020-2759-x
56. Tian Y, Li S, Song J, et al. A doxorubicin delivery platform using engineered natural membrane vesicle exosomes for targeted tumor therapy. *Biomaterials*. 2014;35:2383–2390. doi:10.1016/j.biomaterials.2013.11.083
57. Shtam TA, Kovalev RA, Varfolomeeva EY, et al. Exosomes are natural carriers of exogenous siRNA to human cells in vitro. *Cell Commun Signal*. 2013;11:88. doi:10.1186/1478-811X-11-88
58. Lamichhane TN, Jeyaram A, Patel DB, et al. Oncogene knockdown via active loading of small RNAs into extracellular vesicles by sonication. *Cell Mol Bioeng*. 2016;9:315–324. doi:10.1007/s12195-016-0457-4
59. Alvarez-Erviti L, Seow Y, Yin H, et al. Delivery of siRNA to the mouse brain by systemic injection of targeted exosomes. *Nat Biotechnol*. 2011;29:341–345. doi:10.1038/nbt.1807

60. O'Brien K, Breyne K, Ughetto S, Laurent LC, Breakefield XO. RNA delivery by extracellular vesicles in mammalian cells and its applications. *Nat Rev Mol Cell Biol*. 2020;21:585–606. doi:10.1038/s41580-020-0251-y
61. Opiela J, Bulbul B, Romanek J. Varied approach of using MSCs for bovine embryo in vitro culture. *Anim Biotechnol*. 2020;31:1–8. doi:10.1080/10495398.2018.1448224
62. Ra K, Oh HJ, Kim EY, et al. Comparison of anti-oxidative effect of human adipose- and amniotic membrane-derived mesenchymal stem cell conditioned medium on mouse preimplantation embryo development. *Antioxidants*. 2021;10:268.
63. Welsh JA, Goberdhan DCI, O'Driscoll L, et al. Minimal information for studies of extracellular vesicles (MISEV2023): from basic to advanced approaches. *Journal of Extracellular Vesicles*. 2024;13:e12404. doi:10.1002/jev2.12404
64. Peng G, Suo S, Cui G, et al. Molecular architecture of lineage allocation and tissue organization in early mouse embryo. *Nature*. 2019;572:528–532. doi:10.1038/s41586-019-1469-8
65. Dissanayake K, Nõmm M, Lättekivi F, et al. Oviduct as a sensor of embryo quality: deciphering the extracellular vesicle (EV)-mediated embryo-maternal dialogue. *J Mol Med*. 2021;99:685–697. doi:10.1007/s00109-021-02042-w
66. Nakamura K, Kusama K, Suda Y, et al. Emerging role of extracellular vesicles in embryo-maternal communication throughout implantation processes. *Int J Mol Sci*. 2020;21:5523. doi:10.3390/ijms21155523
67. Es-Haghi M, Godakumara K, Häling A, et al. Specific trophoblast transcripts transferred by extracellular vesicles affect gene expression in endometrial epithelial cells and may have a role in embryo-maternal crosstalk. *Cell Commun Signal*. 2019;17:146. doi:10.1186/s12964-019-0448-x
68. Chen K, Liang J, Qin T, et al. The role of extracellular vesicles in embryo implantation. *Front Endocrinol*. 2022;13:809596. doi:10.3389/fendo.2022.809596
69. Zahir M, Tavakoli B, Zaki-Dizaji M, Hantoushzadeh S, Majidi Zolbin M. Non-coding RNAs in recurrent implantation failure. *Clin Chim Acta*. 2024;553:117731. doi:10.1016/j.cca.2023.117731
70. Lee JY, Ahn EH, Kim JO, et al. Associations between microRNA (miR-25, miR-32, miR-125, and miR-222) polymorphisms and recurrent implantation failure in Korean women. *Hum Genomics*. 2019;13:68. doi:10.1186/s40246-019-0246-y
71. Ahmadi M, Pashangzadeh S, Moraghebi M, et al. Construction of circRNA-miRNA-mRNA network in the pathogenesis of recurrent implantation failure using integrated bioinformatics study. *J Cell Mol Med*. 2022;26:1853–1864. doi:10.1111/jcmm.16586
72. Huang J, Song N, Xia L, et al. Construction of lncRNA-related competing endogenous RNA network and identification of hub genes in recurrent implantation failure. *Reprod Biol Endocrinol*. 2021;19:108. doi:10.1186/s12958-021-00778-1
73. Zhao Y, He D, Zeng H, et al. Expression and significance of miR-30d-5p and SOCS1 in patients with recurrent implantation failure during implantation window. *Reprod Biol Endocrinol*. 2021;19:138. doi:10.1186/s12958-021-00820-2
74. Gerri C, Menchero S, Mahadevaiah SK, Turner JMA, Niakan KK. Human embryogenesis: a comparative perspective. *Annu Rev Cell Dev Biol*. 2020;36:411–440. doi:10.1146/annurev-cellbio-022020-024900
75. Artus J, Chazaud C. A close look at the mammalian blastocyst: epiblast and primitive endoderm formation. *Cell Mol Life Sci*. 2014;71:3327–3338.
76. Fleming TP, McConnell J, Johnson MH, Stevenson BR. Development of tight junctions de novo in the mouse early embryo: control of assembly of the tight junction-specific protein, ZO-1. *J Cell Biol*. 1989;108:1407–1418. doi:10.1083/jcb.108.4.1407
77. Rossant J, Tam PPL. Early human embryonic development: blastocyst formation to gastrulation. *Dev Cell*. 2022;57:152–165. doi:10.1016/j.devcel.2021.12.022
78. Nothias JY, Majumder S, Kaneko KJ, DePamphilis ML. Regulation of gene expression at the beginning of mammalian development. *J Biol Chem*. 1995;270:22077–22080. doi:10.1074/jbc.270.38.22077
79. Hamatani T, Carter MG, Sharov AA, Ko MS. Dynamics of global gene expression changes during mouse preimplantation development. *Dev Cell*. 2004;6:117–131. doi:10.1016/S1534-5807(03)00373-3
80. Johnson MH. From mouse egg to mouse embryo: polarities, axes, and tissues. *Annu Rev Cell Dev Biol*. 2009;25:483–512. doi:10.1146/annurev.cellbio.042308.113348
81. Strauss B, Adams RJ, Papalopulu N. A default mechanism of spindle orientation based on cell shape is sufficient to generate cell fate diversity in polarised Xenopus blastomeres. *Development*. 2006;133:3883–3893. doi:10.1242/dev.02578
82. Piotrowska K, Zernicka-Goetz M. Role for sperm in spatial patterning of the early mouse embryo. *Nature*. 2001;409:517–521. doi:10.1038/35054069
83. Bischoff M, Parfitt DE, Zernicka-Goetz M. Formation of the embryonic-abembryonic axis of the mouse blastocyst: relationships between orientation of early cleavage divisions and pattern of symmetric/asymmetric divisions. *Development*. 2008;135:953–962. doi:10.1242/dev.014316
84. Fleming TP. A quantitative analysis of cell allocation to trophectoderm and inner cell mass in the mouse blastocyst. *Dev Biol*. 1987;119:520–531. doi:10.1016/0012-1606(87)90055-8
85. Strumpf D, Mao C-A, Yamanaka Y, et al. Cdx2 is required for correct cell fate specification and differentiation of trophectoderm in the mouse blastocyst. *Development*. 2005;132:2093–2102. doi:10.1242/dev.01801
86. Sasaki H. Roles and regulations of Hippo signaling during preimplantation mouse development. *Dev Growth Differ*. 2017;59:12–20. doi:10.1111/dgd.12335
87. Mashiko D, Ikeda Z, Tokoro M, et al. Asynchronous division at 4-8-cell stage of preimplantation embryos affects live birth through ICM/TE differentiation. *Sci Rep*. 2022;12:9411. doi:10.1038/s41598-022-13646-8
88. Blázquez R, Sánchez-Margallo FM, Álvarez V, et al. Murine embryos exposed to human endometrial MSCs-derived extracellular vesicles exhibit higher VEGF/PDGF AA release, increased blastomere count and hatching rates. *PLoS One*. 2018;13:e0196080. doi:10.1371/journal.pone.0196080
89. Vilella F, Moreno-Moya JM, Balaguer N, et al. Hsa-miR-30d, secreted by the human endometrium, is taken up by the pre-implantation embryo and might modify its transcriptome. *Development*. 2015;142:3210–3221. doi:10.1242/dev.124289
90. Sidrat T, Khan AA, Joo M-D, et al. Bovine oviduct epithelial cell-derived culture media and exosomes improve mitochondrial health by restoring metabolic flux during pre-implantation development. *Int J Mol Sci*. 2020;21:7589. doi:10.3390/ijms21207589
91. de Alcântara-Neto AS, Cuello C, Uzbekov R, et al. Oviductal extracellular vesicles enhance porcine in vitro embryo development by modulating the embryonic transcriptome. *Biomolecules*. 2022;12:1300. doi:10.3390/biom12091300
92. El-Andaloussi S, Lee Y, Lakhal-Littleton S, et al. Exosome-mediated delivery of siRNA in vitro and in vivo. *Nat Protoc*. 2012;7:2112–2126. doi:10.1038/nprot.2012.131

93. Li H, Huang H, Chen X, et al. The delivery of hsa-miR-11401 by extracellular vesicles can relieve doxorubicin-induced mesenchymal stem cell apoptosis. *Stem Cell Res Ther*. 2021;12:77. doi:10.1186/s13287-021-02156-5
94. Dai H, Luo J, Deng L, et al. Hierarchically injectable hydrogel sequentially delivers antagomiR-467a-3p-loaded and antagomiR-874-5p-loaded satellite-cell-targeting bioengineered extracellular vesicles attenuating sarcopenia. *Adv Healthc Mater*. 2023;12:e2203056. doi:10.1002/adhm.202203056
95. Zhang Y, Chen Y, Shi L, et al. Extracellular vesicles microRNA-592 of melanoma stem cells promotes metastasis through activation of MAPK/ERK signaling pathway by targeting PTPN7 in non-stemness melanoma cells. *Cell Death Discov*. 2022;8:428. doi:10.1038/s41420-022-01221-z
96. Han C, Zhou J, Liu B, et al. Delivery of miR-675 by stem cell-derived exosomes encapsulated in silk fibroin hydrogel prevents aging-induced vascular dysfunction in mouse hindlimb. *Mater Sci Eng C Mater Biol Appl*. 2019;99:322–332. doi:10.1016/j.msec.2019.01.122